An accurate comprehensive approach to substructure – II. Stripped subhaloes

Eduard Salvador-Solé,[1][*] Alberto Manrique[1] and Ignacio Botella[1,2]

[1]*Institut de Ciències del Cosmos, Universitat de Barcelona, Martí i Franquès 1, E-08028 Barcelona, Spain*
[2]*Department of Astronomy, Graduate School of Science, Kyoto University, Kitashirakawa, Oiwakecho, Sakyo-ku, Kyoto 606-8502, Japan*

ABSTRACT

In Salvador-Solé, Manrique & Botella (Paper I), we used the ConflUent System of Peak trajectories (CUSP) formalism to derive from first principles and no single free parameter the accurate abundance and radial distribution of both diffuse dark matter (dDM) and subhaloes accreted on to haloes and their progenitors at all previous times. Here we use those results as initial conditions for the monitoring of the evolution of subhaloes and dDM within the host haloes. Specifically, neglecting dynamical friction, we accurately calculate the effects of repetitive tidal stripping and heating on subhaloes as they orbit inside the host halo and infer the amount of dDM and subsubhaloes they release into the intrahalo medium. We then calculate the expected abundance and radial distribution of stripped subhaloes and dDM. This derivation clarifies the role of halo concentration in substructure and unravels the origin of some key features found in simulations including the dependence of substructure on halo mass. In addition, it unveils the specific effects of dynamical friction on substructure. The results derived here are for purely accreting haloes. In Salvador-Solé et al. (Paper III), we complete the study by addressing the case of low-mass subhaloes, unaffected by dynamical friction, in ordinary haloes having suffered major mergers.

Key words: methods: analytical – galaxies: haloes – dark matter – cosmology: theory.

1 INTRODUCTION

Halo substructure is a subject of paramount importance for its multiple implications in many astrophysical issues. It has thus been amply studied by all available means.

High-resolution *N*-body simulations (e.g. Diemand, Kuhlen & Madau 2007; Springel et al. 2008, hereafter SWV; Angulo et al. 2009; Elahi, Widrow & Thacker 2009; Boylan-Kolchin et al. 2010; Giocoli et al. 2010; Gao et al. 2011, 2012; Klypin, Trujillo-Gomez & Primack 2011; Onions et al. 2012; Cautun et al. 2014; Lovell et al. 2014; Ishiyama et al. 2021) and, more recently, hydrodynamical simulations (Font et al. 2020; Richings et al. 2020; Font, McCarthy & Belokurov 2021; see also Bose et al. 2016, 2020; Hellwig et al. 2016 for the inclusion of gas using a semi-analytic treatment) have allowed to characterize their properties, while analytic models have been used to try to understand the origin of those properties (e.g. Taylor & Babul 2001, 2004; Fujita et al. 2002; Sheth 2003; Zentner & Bullock 2003; Lee 2004; Oguri & Lee 2004; Peñarrubia & Benson 2005; van den Bosch, Tormen & Giocoli 2005; Zentner et al. 2005; Kampakoglou & Benson 2007; Giocoli, Tormen & van den Bosch 2008; Benson et al. 2013; Pullen, Benson & Moustakas 2014; Griffen et al. 2016; Jiang & van den Bosch 2016; van den Bosch & Jiang 2016).

The modelling of substructure is particularly hard. One must account for the rate at which haloes of different masses are accreted on to the host halo and converted into subhaloes, determine their initial radial and velocity distributions, and monitor their fate as they orbit inside the host halo. Subhaloes neither accrete gas (all

cooled gas goes to the centre of the halo) nor merge with each other (they have too large relative velocities; Angulo et al. 2009) nor even suffer significant harassment (van den Bosch et al. 2018). But they are tidally stripped and heated by the potential well of the host halo in a complicate way that depends not only on their initial location and velocity, but also on their varying mass and concentration. In addition, the host haloes themselves have different assembly histories, which translate into different evolving histories of subhaloes. It is thus not surprising that, despite all the efforts gone on this study using both (semi)analytic models plus numerical experiments (e.g. van den Bosch & Jiang 2016; van den Bosch et al. 2018; Green & van den Bosch 2019; Jiang et al. 2021) and simulations (e.g. Ghigna et al. 1998; Hayashi et al. 2003), the origin of the characteristic properties of substructure remains an open issue.

One interesting result along this line of research was obtained by Han et al. (2016, hereafter HCFJ). These authors showed that the properties of subhaloes found in simulations are encoded in the following three conditions: (1) the scaled number density profiles of subhaloes with original mass M_s that were accreted on to the halo or its progenitors at all previous times overlap in one curve proportional to the scaled density profile of the host halo; (2) the cumulative mass function (MF) of such accreted subhaloes is a power law with logarithmic slope, $d\mathcal{N}(> M_s)/d \ln M_s$, close to -1; and (3) the truncated-to-original mass ratio of the final stripped subhaloes only depends on their radial distance to the centre of the halo. Strictly speaking, the two first conditions refer to 'unevolved' rather than 'accreted' subhaloes, but both kinds of subhaloes coincide for subhaloes with low enough masses unaffected by dynamical friction (see Salvador-Solé, Manrique & Botella 2021, hereafter Paper I). Unfortunately, what causes these conditions is unknown.

[*] E-mail: e.salvador@ub.edu

With the aim to shed light on this issue, a novel approach was applied in Paper I making use of the so-called ConflUent System of Peak trajectories (CUSP) formalism (Manrique & Salvador-Solé 1995, 1996; Manrique et al. 1998). CUSP is a powerful analytic formalism that, by monitoring the collapse and virialization of halo seeds, i.e. peaks (or maxima) in the Gaussian random field of density perturbations (Juan et al. 2014a), allows one to infer *from first principles and with no single free parameter* all macroscopic halo properties, namely the MF (Juan et al. 2014b) and the mean spherically averaged density (Salvador-Solé et al. 2012a), velocity dispersion and anisotropy profiles, and the prolateness and ellipticity profiles (Salvador-Solé et al. 2012b, hereafter SSMG). Not only are the predictions in full agreement with the results of simulations in both cold dark matter (CDM; all previous references) and warm dark matter (WDM; Viñas, Salvador-Solé & Manrique 2012) cosmologies, but their derivation clarifies the origin of all these properties and their characteristic features. A comprehensive review of CUSP and its achievements is given in Salvador-Solé & Manrique (2021).

In Paper I, we extended the domain of application of CUSP to the basic halo components: diffuse dark matter (dDM) and subhaloes. We derived the MF and radial distribution of accreted subhaloes that allowed us to explain the origin of the two first above-mentioned HCFJ conditions. In this paper, we use those results as initial conditions for the study of the fate of dDM and subhaloes within the host haloes. For simplicity, we concentrate on haloes evolving by pure accretion, which is enough to explain the third HCFJ condition. The more realistic though complicated case of ordinary haloes having suffered major mergers is postponed to Salvador-Solé et al. (2021, hereafter Paper III).

The layout of this paper is as follows. In Section 2, we remind the results of Paper I. In Section 3, we carefully model tidal stripping of subhaloes by the host potential well. The abundance and radial distribution of stripped subhaloes and of dDM are derived in Sections 4 and 5, respectively, under the approximation that all subhaloes have similar concentrations. In Section 6, we relax that approximation and analyse the dependence of substructure on halo mass. Our results are summarized and discussed in Section 7.

Throughout this paper our predictions are calculated for current Milky Way (MW)-like haloes with virial mass, i.e. the mass out to the radius encompassing an inner mean density equal to the virial overdensity (Bryan & Norman 1998; Henry 2000) times the mean cosmic density, of $M_h = 2.2 \times 10^{12}$ M$_\odot$, which according to Salvador-Solé & Manrique (2021) correspond to the maximum extend of the virialized part of haloes. These predictions are compared to the results for the same kinds of haloes studied by HCFJ or SWV, who use the masses $M_{200} = 1.84 \times 10^{12}$ M$_\odot$ or $M_{50} = 2.5 \times 10^{12}$ M$_\odot$, respectively, i.e. out to the radius encompassing an inner mean density of 200 or 50 times the critical cosmic density. The cosmology adopted is the 7-year Wilkinson Microwave Anisotropy Probe (*WMAP*7) cosmology (Komatsu et al. 2011) as in those latter works. The CDM spectrum we use is according to the prescription given by Bardeen et al. (1986) with the Sugiyama (1995) shape parameter.

Given that in this paper we deal with both stripped and accreted subhaloes, all properties referring to the former are denoted with superindex 'stp', whereas those referring to the latter, derived in Paper I, are denoted with superindex 'acc'.

2 ACCRETED SUBHALOES

The main results of Paper I are summarized next (see that paper for details).

(i) There is a one-to-one correspondence between haloes with mass M_h at the time t_h and their seeds, non-nested peaks with density contrast δ at the scale S, in the Gaussian random field of density perturbations at an arbitrary initial time t_i smoothed with a Gaussian window. See Paper I for the functions $\delta(t_h)$ and $S(M_h, t_h)$ corresponding to the cosmology and halo mass definition of interest.

(ii) Consequently, the continuous time evolution of accreting haloes is traced by continuous peak trajectories in the δ–S plane at t_i. Those continuous trajectories are interrupted in major mergers, where new continuous peak trajectories arise tracing the evolution of the haloes arising from the mergers.

(iii) The previous correspondence yields in turn another one-to-one correspondence between subhaloes of mass M_s accreted by the halo (or any of its progenitors) at any time $t \leq t_h$ and peaks with $\delta(t)$ at the scale $S(M_s)$ that become nested in the peak with the same density contrast at a larger scale associated with the host halo.

(iv) When a halo is accreted on to another halo and becomes a subhalo, its associated peak becomes nested in the peak tracing the host halo. On the other hand, nested peaks are preserved like subhaloes when haloes suffer major mergers. Thus, the dynamical evolution of subhaloes of any level can be monitored through the filtering evolution of nested peaks of the same level in the δ–S plane.

(v) For the reasons explained in Salvador-Solé & Manrique (2021), the properties of haloes including those regarding accreted subhaloes do not depend on their assembly history. In other words, they do not depend on whether haloes undergo monolithic collapse (pure accretion) or lumpy collapse (including major mergers). Consequently, to derive all these properties we have the right to assume pure accretion with no loss of generality.

(vi) During accretion phases haloes grow inside-out, i.e. shells accreted at a time $t(r)$ when the halo reached the mass $M(r)$,[1] are deposited at the radius r without altering the inner structure of the halo. By 'deposited at r' we mean that the subhalo orbits stabilize with their apocentre at that radius.

(vii) The orbits of subhaloes accreted at $t(r)$ are determined by their random (tangential) velocities v at their apocentre at r, which arise from the collapse and virialization of the halo,[2] so they do not depend on the subhalo mass M_s.

(viii) The inside-out growth of purely accreting haloes allows one to derive their mean spherically averaged density profile and the abundance and mean spherically averaged number density profile per infinitesimal mass of accreted subhaloes from the abundance of nested peaks arising from Gaussian statistics.

(ix) CUSP also accounts for the dDM outside haloes arising from the existence of a minimum halo mass due to the free-streaming mass associated with weakly interacting massive particles (WIMPs) in the real Universe or the halo resolution mass in simulations. When this dDM is accreted on to haloes, it gives rise to a non-null dDM mass fraction, $f_{dDM}^{acc}(r)$, at each radius r of haloes.

3 TIDAL STRIPPING AND HEATING

To infer the properties of substructure regarding stripped subhaloes, we must first determine the effects of tidal stripping and heating on accreted subhaloes orbiting inside the accreting host halo. For

---

[1]$t(r)$ is given by the trajectory $\delta(S)$ tracing the halo growth, with the relations $\delta(t)$ and $S(M_h, t)$ defining the halo-peak correspondence, and the mass profile $M(r)$ of the halo (see Paper I).

[2]The virial relation we refer to throughout this paper includes the external pressure term, so by virialized haloes we simply mean relaxed ones.

simplicity in the calculation of subhalo orbits, we will assume all objects spherically symmetric. This makes a difference with respect to Paper I. In that paper the results obtained, in the form of mean spherically averaged profiles, held for real haloes with different ellipsoidal shapes. Here, instead, the results we will obtain strictly hold for spherically symmetric systems only. None the less, they should hopefully be a good approximation for all haloes duly spherically averaged.

3.1 Truncation

The truncated mass $M_s^{tr}(v, r, M_s)$ of subhaloes with original mass M_s can be calculated from their density profile (see below) and the truncation radius $R_s^{tr}(v, r, M_s)$.

At present there is no consensus about how to estimate the truncation radius (see the detailed discussion in van den Bosch et al. 2018). The most usual procedure is to adopt the tidal-limited radius of the subhalo in a circular orbit at r, i.e. the radius of the subhalo in equilibrium within the tidal field of the host halo at that radius. But even this can be done in several ways, depending on whether or not the centrifugal force (e.g. King 1962; Spitzer 1978; Tormen, Diaferio & Syer 1998; Binney & Tremaine 2008; Tollet et al. 2017) or resonant effects (Klypin, Gottöber & Kravtsov 1999) are taken into account, none of them being fully accurate (Read et al. 2006; Binney & Tremaine 2008; Mo, van den Bosch & White 2010). However, we do not need any accurate value of the truncation radius. For our purposes here it is sufficient to consider that all the previous procedures lead to similar results: the truncation radius encompasses an inner mean density of the subhalo at r, $\bar{\rho}_{[M_s, t(r)]}$, of the order of the mean inner density of the host at radius r, $\bar{\rho}(r)$ (e.g. Hayashi et al. 2003; Diemand et al. 2007; Peñarrubia, Navarro & McConnachie 2008),

$$\bar{\rho}_{[M_s, t(r)]}[R_s(r, M_s)] \approx \bar{\rho}(r). \tag{1}$$

To write equation (1) we have used that accreted subhaloes with apocentre at r were accreted there so that the truncation radius is but the subhalo original radius R_s at accretion. Hereafter, a bar on a function of r denotes the corresponding mean value inside that radius and subindex $[M, t]$ on a (sub)halo property means that the object has a mass M at the time t. However, in the case of the accreting host halo we drop, for simplicity, the subindex $[M_h, t_h]$ or $[M(r), t(r)]$.

However, this is not the whole story because subhalo orbits are not circular but elliptical in general. Thus, the truncation radius of subhaloes varies over their orbit, from the one set at the apocentric radius r where stripping is less intense, well approximated by the relation (1), to that set at the pericentric radius r_{per} where stripping is maximum. In fact, given that subhaloes have large velocities at pericentre, to calculate the truncation radius there it is preferable to use the impulse approximation (Spitzer 1958). But, again, we do not need to derive the accurate truncation radius according to the mass loss calculated in the impulsive approximation (e.g. Gnedin & Ostriker 1999; van den Bosch et al. 2018). For our purposes here it is enough the result found by González-Casado, Mamon & Salvador-Solé (1994) that $R_s^{tr}(v, r, M_s)$ also encompasses a mean inner density in the subhalo of the order of that of the host at $r_{per}(v, r)$,

$$\bar{\rho}_{[M_s, t(r)]}[R_s(r, M_s)Q_s(v, r, M_s)] \approx \bar{\rho}[r_{per}(v, r)], \tag{2}$$

where $Q_s(v, r, M_s)$ stands for their scaled truncated radius, $R_s^{tr}(v, r, M_s)/R_s(r, M_s)$. We remark that the truncation in the impulsive approximations is not directly due to the local tidal field, but to the heating produced in the subhalo at its rapid passage by pericentre, which causes a more marked stripping to the subhalo.

This is why this process is often referred as 'tidal heating' or 'shock heating'. In this work we call 'truncation' the stripping produced in any of these two extreme ways, via tidal limiting radius or via shock heating (or any mixture of them), and call 'heating' the small energy increase that affects the part of the subhalo that remains bound after being truncated.

After being stripped and heated at pericentre, all over their way back to the apocentre, subhaloes tend to reach a new equilibrium state limited by the tidal field at each point. As a consequence, subhaloes can be stripped not only in the first half of their orbits, with an ever increasing tidal field, but possibly also in the second half (this depends on how quick is the response of the system to any previous truncation). However, as the stripping is maximum and much stronger via shock heating at pericentre than via tidal limitation at any other point of the orbit, we adopt for simplicity the viewpoint that the whole truncation (and heating) is concentrated at the pericentre and that, at apocentre, subhaloes just reaccommodate their structure according to the halo mean inner density there. We remark, however, that this simplification should have no practical consequence because, as shown below, we will make sure that the total mass loss produced in any orbit is according to the results of simulations.

Equations (2) and (1) lead to

$$\frac{\bar{\rho}_{[M_s, t(r)]}[R_s(r, M_s)Q_s(v, r, M_s)]}{\bar{\rho}_{[M_s, t(r)]}[R_s(r, M_s)]} \approx \frac{\bar{\rho}[r_{per}(v, r)]}{\bar{\rho}(r)}. \tag{3}$$

Lastly, using the expression

$$\frac{M_s^{tr}(v, r, M_s)}{M_s} = \frac{f[c_s(r)Q_s(v, r, M_s)]}{f[c_s(r)]} \tag{4}$$

holding for subhaloes with the original Navarro–Frenk–White (NFW) density profile (Navarro, Frenk & White 1997) with concentration $c_s(r)$ and the similar expression for the mass ratio $M[r_{per}(r, v)]/M_h$ holding for the host, the relation (3) takes the form

$$\frac{f[c_s(r)Q_s(v, r, M_s)]}{f[c_s(r)][Q_s(v, r, M_s)]^3} = \frac{f[c(r)Q(v, r)]}{f[c(r)][Q(v, r)]^3}, \tag{5}$$

where $Q(v, r)$ stands for $r_{per}(v, r)/r$ and $c(r)$ is the concentration of the accreting halo with mass $M(r)$, and $f(c)$ is defined as $\ln(1 + c) - c/(1 + c)$ (see e.g. Salvador-Solé et al., in preparation for the Einasto profile; Einasto 1965). For simplicity, the uncertainty factor of order unity has been taken equal to 1.

Once the truncation radius or, equivalently, the ratio $Q_s(v, r)$ is known, equation (4) gives the truncated mass $M_s^{tr}(v, r, M_s)$. Note that, for subhaloes accreted at r with similar concentrations $c_s(r)$, equation (5) implies that Q_s does not depend on M_s, i.e. $Q_s(v, r, M_s) \equiv Q_s(v, r)$. Consequently, the mass ratio M_s^{tr}/M_s given in equation (4) and its mean or median value over v are independent of M_s.

3.2 Heating

However things are not that simple. When subhaloes settle in a new equilibrium state at apocentre, their density profiles adopt again the NFW form (SWV) with a somewhat larger concentration c_s^{tr} due to the heating produced at pericentre. Therefore, they will be further stripped and heated at the next orbit and so on so forth. In other words, stripping and heating is a repetitive process.

To calculate the mass loss produced in the next orbit we must determine the new concentration c_s^{tr}, which in turn depends on the heating produced in the previous orbit. In the impulsive approximation, such a heating mostly affects the outer regions of the subhalo, i.e. those which are precisely lost, while the energy of the innermost regions is

rather an adiabatic invariant (Spitzer 1978; Weinberg 1994; Gnedin & Ostriker 1999; van den Bosch et al. 2018) so that the energy gain of the non-truncated part of the system is quite limited. Taking into account the form of the total energy for subhaloes with the NFW density profile, we then arrive at the expression

$$\frac{h\left[c_s^{tr}(v,r)\right]}{h[c_s(r)]} = U(v,r)\left[\frac{M_s^{tr}(v,r,M_s)}{M_s}\right]^{5/6}, \quad (6)$$

where $h(c)$ is defined as $f(c)(1+c)/\{c^{3/2}[3/2-s^2(c)]^{1/2}\}$, being $s^2(c)$ the isotropic 3D velocity variance scaled to $cf(c)GM/R$ of a halo with mass M, radius R, and concentration c, and $U(v,r)$ is the ratio between the total energies after and before the tidal shock of the part of the subhalo *that remains bound*. Thus $U(v,r)$ should be a function of order unity of the strength of the shock or, equivalently, of the subhalo truncated-to-original mass ratio. But the adiabatic shielding against heating in the inner part of subhaloes suffering the shock makes it hard to calculate it accurately. van den Bosch et al. (2018) provide an approximate expression for the ratio between the total energies of the subhalo after and before the shock, but those energies refer to the whole system, not to the part that remains bound. We thus assume, for simplicity, that in the relevant range of subhalo orbits $U(v,r)$ can be approximated by a power law,

$$U(v,r) = K\left[\frac{M_s^{tr}(v,r,M_s)}{M_s}\right]^\beta. \quad (7)$$

The positive constant of order one K and the negative index with small absolute value β will be adjusted below by comparing the predictions of this model to the results of numerical simulations. Note that, unless K is exactly equal to unity, the approximation (7) cannot be valid for orbits close to circular because $M_s^{tr}(v,r,M_s)/M_s$ and $U(v,r)$ should then approach unity in parallel. Fortunately, subhaloes with nearly circular orbits are very rare (Tormen 1997; Zentner et al. 2005; Wetzel 2011), so this slight flaw of the model should have a negligible effect in the results. In any event, disregarding its exact form, the function U cannot depend on M_s because $M_s^{tr}(v,r,M_s)/M_s$ does not, so c_s^{tr}/c_s does not depend on M_s either (see equation 6).

3.3 Repetitive stripping

To calculate the final truncated mass of subhaloes with original mass M_s accreted at $t(r)$ on to a purely accreting halo with M_h at t_h, we must monitor the changes produced in subhaloes at every pericentric passage between $t(r)$ and t_h in an iterative way. The result will depend of course on the concentration $c(r)$ of the host halo at $t(r)$ inside which subhaloes accreted at that time orbit and on the initial properties of those subhaloes.

Given the inside-out growth of the host halo, $c(r)$ is simply r/r_s, where r_s is the core radius of the halo at the final time t_h. Regarding subhaloes, after turnaround they fall on to the halo and start orbiting and being stripped and heated, so their mass M_s when their apocentre is stabilized at r is somewhat smaller than the mass M_s^{ntr} they would have had they evolved as free (non-accreted) haloes until $t(r)$. Since during virialization subhalo velocities vary randomly independently of their mass, all subhaloes at r must have the same velocity distribution (Jiang et al. 2015). Thus we can derive their typical scaled truncation radius Q_s from equation (5) from the initial subhalo concentration c_s^{ntr} given by the M–c relation for M_s^{ntr} at $t(r)$ and the function $Q(r)$ equal to twice the velocity-average value

obtained of subhaloes at r and $t(r)$.[3] Then, plugging the solution Q_s in equation (4), we obtain M_s/M_s^{ntr} and, using equations (6) and (7), we are led to the concentration c_s of accreted subhaloes.

According to the results of Section 3.1, provided all haloes with different masses M_s^{ntr} accreted at $t(r)$ had similar concentrations c_s^{ntr}, the mass ratio M_s/M_s^{ntr} would be a function independent of M_s^{ntr}, hereafter denoted as $m(r)$, and so would also Q_s and c_s. The derivation followed next makes that approximation in order to catch the main effect of subhalo stripping; the slight dependence on subhalo concentration on mass will be addressed in Section 6. Since this derivation uses an iterative procedure, it is convenient to denote the initial properties $M_s(r,M_s^{ntr})$, $Q_s(r)$, and $c_s(r)$ of accreted subhaloes as $M_0(r,M_s^{ntr})$ (with $M_0(r,M_s^{ntr}) < M(r)/3$; see Paper I), $Q_0(r)$, and $c_0(r)$, respectively, and increase the subindex in one unit at each new orbit.

At first pericentric passage after $t(r)$, subhaloes are truncated at the scaled truncation radius $Q_1(v,r)$ given by equation (5) and acquire the mass $M_1(v,r,M_s^{ntr})$ given by equation (4) or, taking into account equation (5) also holding for M_0/M_s^{ntr}, by the relation

$$\frac{M_1\left(v,r,M_s^{ntr}\right)}{M_0\left(r,M_s^{ntr}\right)} = \frac{M_0\left(r,M_s^{ntr}\right)}{M_s^{ntr}}\left[\frac{Q_1(v,r)}{Q_0(r)}\right]^3. \quad (8)$$

As M_0/M_s^{ntr} does not depend on M_s^{ntr} (see the discussion above), M_1/M_0 does not either. Then, equation (6) leads to the new concentration $c_1(v,r)$ when subhaloes reach apocentre.

Similarly, at second and successive passages, subhaloes with M_i, Q_i, and c_i are truncated at the scaled truncation radius $Q_{i+1}(v,r)$ given by

$$\frac{f[c_i(v,r)Q_{i+1}(v,r)]}{f[c_i(v,r)]Q_{i+1}^3(v,r)} = \frac{f[c(r)Q(v,r)]}{f[c(r)]Q^3(v,r)}, \quad (9)$$

leading to a mass M_{i+1} satisfying

$$\frac{M_{i+1}\left(v,r,M_s^{ntr}\right)}{M_i\left(v,r,M_s^{ntr}\right)} = \frac{M_i\left(v,r,M_s^{ntr}\right)}{M_{i-1}\left(v,r,M_s^{ntr}\right)}\left[\frac{Q_{i+1}(v,r)}{Q_i(v,r)}\right]^3, \quad (10)$$

and to a concentration c_{i+1} according to

$$\frac{h[c_{i+1}(v,r)]}{h[c_i(v,r)]} = K\left[\frac{M_{i+1}\left(v,r,M_s^{ntr}\right)}{M_i\left(v,r,M_s^{ntr}\right)}\right]^{\beta+5/6}. \quad (11)$$

This iterative process leads to a total truncated mass M_s^{tr} at t_h of subhaloes with original mass $M_0 = M_s$ and scaled truncation radius $Q_0 = Q_s$ equal to

$$\frac{M_s^{tr}\left(v,r,M_s^{ntr}\right)}{M_s\left(r,M_s^{ntr}\right)} = m^\nu(r)\prod_{i=1}^{\nu}\left[\frac{Q_i(v,r)}{Q_s(r)}\right]^3, \quad (12)$$

where $\nu > 0$ is the total number of constant orbits achieved by subhaloes from $t(r)$ to t_h.

As shown in Fig. 1, for $K = 0.77$ and $\beta = -1/2$, the predictions of the model for a wide range of orbits recover the results of numerical simulations by Hayashi et al. (2003). As the best value of K is smaller than unity, to avoid an artificial cooling in nearly circular orbits, i.e. when M_s^{tr}/M_s approaches unity, we take from now on the expression (7) bounded to unity.

---

[3] According to the spherical collapse model (Bryan & Norman 1998) justified by CUSP (Salvador-Solé & Manrique 2021), subhalo apocentric radii typically shrink a factor of 2 since turnaround, so do also their pericentric radius r_{per}, implying that r_{per}/r for subhaloes at r was typically a factor of 2 larger before being accreted.
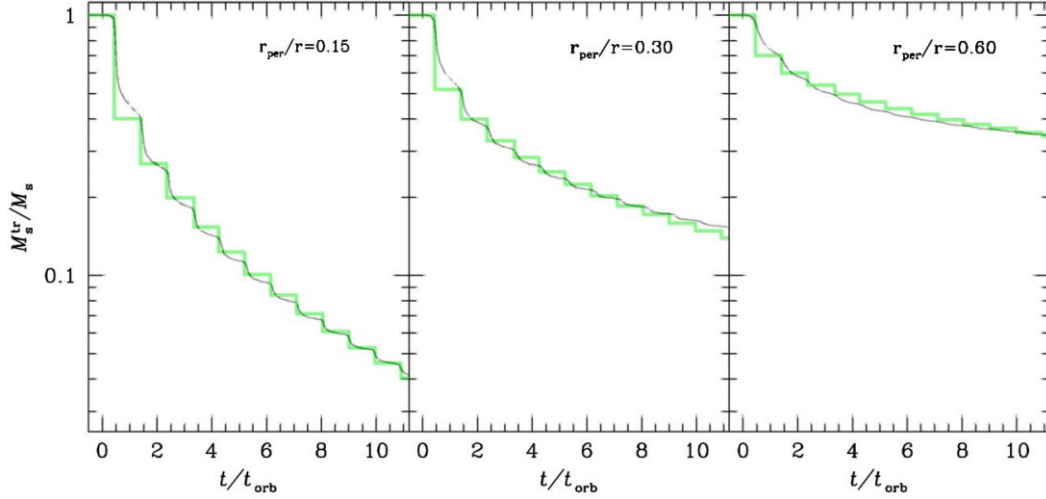
Figure 1. Predicted mass evolution of subhaloes with the NFW density profile and suited concentrations c_s (green lines) suffering repetitive tidal stripping and shock-heating within a halo also with the NFW density profile and concentration $c(r) = 10$ for three different values of $r_{per}(v, r)/r$, compared to the results of a dedicated numerical experiment (thin black lines) performed by Hayashi et al. (2003). The smoother shape of the empirical curves is due to the actual progressive stripping and response of subhaloes to the conditions found over the orbits, while the theoretical predictions focus on the maximum stripping taking place at the pericentre and the recovery of equilibrium of the system at apocentre.

Equation (12) tells that the truncated-to-original mass ratio M_s^{tr}/M_s does not depend on M_s and the same is true for its mean (or median) value over v. We thus see that the reason for HCFJ condition 3 in the realistic case of repetitive stripping is the same as in single orbits: the *similar* concentration of subhaloes at accretion and the fact that subhaloes at r are truncated at the radius encompassing a mean inner density of the order of that of the host halo at r.

3.4 Disruption

The possibility that subhaloes can be fully disrupted as a consequence of tidal stripping is not clear. Hayashi et al. (2003) pointed out that the total energy of subhaloes endowed with a NFW density profile can become positive after truncation so that they can be disrupted. However, van den Bosch et al. (2018) showed that, when a subhalo is being stripped, its structure quickly responds to the departure from equilibrium so that the total energy of the new truncated system is not simply that of the part of the initial system out to the effective truncation radius. Moreover, even if the system could not immediately respond to stripping, the total energy of a severely truncated subhalo with the NFW profile would only become positive provided its velocity distribution was strongly tangential, while in real (sub)haloes it is radially biased.

According to these arguments, the full disruption of subhaloes would be a very rare event. However, numerical simulations do find a significant disruption above the subhalo resolution mass. Whether it is due to overmerging or any other numerical artefact as claimed by van den Bosch et al. (2018) is not clear. In any event, if we are to compare our theoretical predictions to the results of simulations, we must account for it. Therefore, we will consider two scenarios: one with negligible disruption and another one with disruption, less marked than in the isotropic case though. The rest of this section is devoted to this latter scenario.

The pericentric radius $r_{per} \equiv rQ(v, r)$ of a subhalo is related to its tangential velocity v at the apocentre through

$$v^2 = 2 \left\{ \frac{\Phi(r) - \Phi[rQ(v, r)]}{1 - Q^2(v, r)} \right\}, \tag{13}$$

where $\Phi(r) = -GM(r)/r \ln[1 + c(r)]/f[c(r)]$ is the potential of the host at r. To leading order, equation (13) leads to

$$Q(v, r) = \frac{1}{2} \frac{rv^2}{GM(r)}. \tag{14}$$

Since accreted subhaloes become increasingly resistant to disruption due to the increase of their concentration at each passage by the pericentre. Since, they can only be disrupted at first pericentre passage when their concentration is $c_0(r)$. Assuming that the condition for disruption for subhaloes with concentration c_s is $R^{tr}/R \equiv Q_s \sim 0.5/c_s$,[4] equation (5), with $c_s = c_0(r)$ and Q_s given by equation (14), leads to a tangential velocity for disruption at r, $v_{dis}(r)$, satisfying the relation

$$\frac{f[c_0(r)]}{f(0.5)}[1 + c(r)]^2 \left[\frac{rv_{dis}^2(r)}{2GM(r)}\right]^3 - c^2(r)\frac{rv_{dis}^2(r)}{2GM(r)} - 1 = 0. \tag{15}$$

We thus see that $v_{dis}(r)$ is independent of M_0 (and M_s). From equations (14) and (15) we also have that the minimum pericentric radius for surviving subhaloes is

$$r_{per}^{min} = r \frac{f[c_0(r)]}{f(0.5)} \left[\frac{0.5}{c_0(r)}\right]^3. \tag{16}$$

The fraction of accreted subhaloes with original mass M_s that are destroyed, $f_{dis}(r, M_s)$, is thus equal to the integral of velocity distribution function, $\mathcal{N}(v, r, M_s)$ up to $v_{dis}(r)$ divided by the same integral up to $v_{max}(r) = [GM(r)/r]^{1/2}$, i.e. the maximum possible value of v for subhaloes with apocentre at r. For any reasonable (mass-independent) tangential velocity distribution of subhaloes accreted at r, in particular that mentioned in Section 4, we arrive to leading order at the following M_s-independent disruption fraction:

$$f_{dis}(r) = \frac{v_{dis}^2(r)}{v_{max}^2(r)} = \frac{rv_{dis}^2(r)}{GM(r)}, \tag{17}$$

---

[4]The critical value for disruption found by Hayashi et al. (2003) for isotropic NFW subhaloes is $0.77/c_s$.

where $v_{dis}(r)$ is the solution of equation (15). Note that $f_{dis}(r)$ is independent of the subhalo mass.

4 RADIAL DISTRIBUTION AND MASS FUNCTION OF STRIPPED SUBHALOES

As shown in Salvador-Solé & Manrique (2021), the virialization taking place in a major merger yields the memory loss of the system, so the inner properties of the final relaxed object, including those regarding accreted haloes, do not depend on its assembly history. Taking advantage of this important conclusion, in Paper I we concentrated on purely accreting haloes, which notably simplified the calculations without affecting the general validity of the results. Unfortunately, the situation regarding stripped subhaloes is very different. Tidal stripping brakes that possibility because its effects on individual subhaloes are not erased by virialization, so stripped haloes retain the memory of their past history. As a consequence, to derive the properties of substructure regarding stripped subhaloes we must account for the assembly history of their host haloes.

In the rest of this paper we concentrate on the simplest case of purely accreting haloes or, more exactly, of haloes having been accreting for a long time.[5] The more complex case of haloes having suffered recent major mergers is addressed in Paper III.

In these conditions, the mean number of stripped subhaloes per infinitesimal truncated mass and radius within a halo with mass M_h (and virial radius R_h) at t_h is

$$\mathcal{N}^{stp}\left(r, M_s^{tr}\right) = \mathcal{N}^{tr}\left(r, M_s^{tr}\right) + \int_{v_{dis}(r)}^{v_{max}(r)} dv \int_{M_s}^{M(r)} dM$$
$$\times \mathcal{N}^{acc}(v, r, M) \int_{R^{tr}(v,r,M)}^{R(r,M)} dr' \mathcal{N}^{stp}_{[M,t(r)]}\left(r', M_s^{tr}\right),$$
(18)

where $\mathcal{N}^{stp}_{[M,t(r)]}(r', M_s^{tr})$ is the abundance of stripped subsubhaloes at r' inside subhaloes with M accreted at $t(r)$. The first term on the right-hand side of equation (18), $\mathcal{N}^{tr}(r, M_s^{tr})$, gives the mean abundance of stripped subhaloes directly arising from the *truncation* of subhaloes accreted at r with suited original mass,

$$\mathcal{N}^{tr}\left(r, M_s^{tr}\right) = \int_{v_{dis}(r)}^{v_{max}(r)} dv \, \mathcal{N}^{acc}\left[v, r, M_s\left(v, r, M_s^{tr}\right)\right]$$
$$\times \frac{\partial M_s\left(v, r, M_s^{tr}\right)}{\partial M_s^{tr}}.$$
(19)

The second term gives the abundance of stripped subhaloes with M_s^{tr} that arise from subsubhaloes at r' between the non-truncated radius $R(r, M)$ and truncated one $R^{tr}(v, r, M)$ of subhaloes with masses M between M_s and $M(r)$ at $t(r)$, $\mathcal{N}^{stp}_{[M,t(r)]}(r', M_s^{tr})$. Note that we take into account that such released subsubhaloes are not further stripped in the host halo (see Appendix B).

As the kinematics of objects with apocentre at r does not depend on their mass (see Section 3), the abundance $\mathcal{N}^{acc}(v, r, M_s)$ of accreted subhaloes per infinitesimal original mass, radius, and (tangential) velocity in equation (21) factorizes in the velocity distribution (Jiang et al. 2015) times the mean abundance of accreted subhaloes, $\mathcal{N}^{acc}(r, M_s)$, equal to (equation 17 of Paper I)

$$\mathcal{N}^{acc}(r, M_s) = 4\pi r^2 \frac{\rho(r)}{M_h} \mathcal{N}^{acc}(M_s),$$
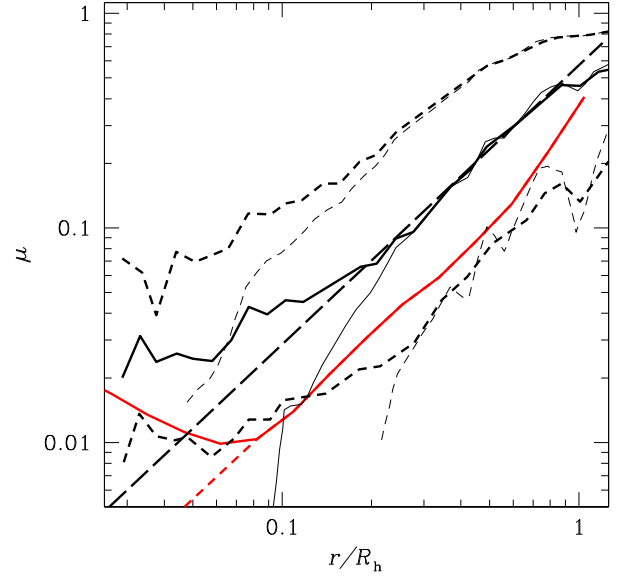(20)

Figure 2. Mean truncated-to-original subhalo mass ratio profile predicted for purely accreting MW-mass haloes (solid red line) for subhaloes with concentrations equal to that of haloes with $10^{-2}M(r)$ at $t(r)$ according to the empirical M–c relation by Gao et al. (2008). For comparison we plot the empirical *median* mass ratio profile of resolved (thick black lines) and resolved plus orphan (thin black lines) subhaloes found by HCFJ in the Level 1 Aquarius halo A (thin and thick dashed black lines give the corresponding upper/lower 1σ percentiles, respectively), which has been accreting since $r = 0.08R_h$. We also plot the power-law *median* profile of index 1.3 used in the HCFJ model (long-dashed black line) and the power-law extrapolation of our theoretical mean profile (dashed red line) at the radius $r < 0.08R_h$, from which the halo A has evolved by accretion as considered in our model.

if $M_s < M(r)/3$ and zero otherwise. Thus, taking into account that the MF of accreted subhaloes $\mathcal{N}^{acc}(M_s)$ is very nearly proportional to M_s^{-2} (Paper I), equation (19) leads to the simple expression

$$\mathcal{N}^{tr}\left(r, M_s^{tr}\right) = \mu(r)\mathcal{N}^{acc}\left(r, M_s^{tr}\right),$$
(21)

where $\mu(r)$ stands for the average over v from zero (or $v_{dis}(r)$ in case of significant disruption; see Section 3.4) to $v_{max}(r)$ of the truncated-to-original mass ratio M_s^{tr}/M_s of subhaloes with original mass $M_s < M(r)/3$ at r.[6] Note that, $\mathcal{N}^{acc}(r, M_s^{tr})$ is separable (equation 20), so is also $\mathcal{N}^{tr}(r, M_s^{tr})$.

The $\mu(r)$ profile can be readily calculated by monitoring the mass loss through repetitive stripping and heating (equation 12) of accreted subhaloes with suited initial properties (see Section 3) and taking the velocity averages for the velocity distribution function given in Appendix C. The typical concentration of subhaloes accreted by the host halo at $t(r)$ is taken equal to that of haloes with $10^{-2}M(r)$ at that time according to the (time-varying) M–c relation found by Gao et al. (2008) in simulations similar to those used by SWV and HCFJ. The result is very little sensitive, however, to the particular subhalo mass chosen provided it is between $10^{-1}M(r)$ and $10^{-3}M(r)$.

The resulting $\mu(r)$ profile, which coincides down to one thousandth R_h for the cases of null or moderate disruption, is shown in Fig. 2. For comparison we also plot the results found by HCFJ for the MW-mass halo A in the Level 1 (maximum resolution) Aquarius simulation (SWV). Note that this halo is particularly well suited to

---

[5]See Paper I for the relation between the time of the last major merger and the radius from which the object has grown inside-out.

[6]By $\mathcal{N}^{acc}(M_s^{tr})$ we mean $\mathcal{N}^{acc}$ for a value of the accreted subhalo mass equal to M_s^{tr}.

the comparison with the predictions of CUSP for purely accreting haloes because it has been accreting since $z \sim 6$, i.e. it has been growing inside-out from $r/R_h \sim 0.08$ (see fig. 1 of Paper I). Thus, the comparison is only meaningful down to that radius. To see how sensitive the results are on the modelling below $r = 0.08R_h$, we also consider the theoretical $\mu(r)$ profile extrapolated by a simple power law to small radii. Of course, we cannot pretend that the predicted $\mu(r)$ profile coincides with that found by HCFJ in the A halo: ours refers to the *mean* truncated-to-original subhalo mass ratio, while HCFJ's refers to the *median* one. More importantly, as mentioned in Paper I, the μ profile derived by HCFJ is for subhaloes of all levels, while ours holds for first-level subhaloes only. Since these latter are the only subhaloes being stripped, including all level subhaloes should notably enhance the resulting mass ratio. This would explain that our mean μ profile is substantially lower than the median μ profile found by HCFJ, contrarily to what would be expected for a lognormal distribution of mass ratios referring to the same subhalo population. Note also that the validity of our mean profile is supported by the fact that, as we will see, it leads to the right amplitude of the predicted MF of stripped subhaloes. On the contrary, were the predicted mean $\mu(r)$ profile raised to at least the position of the empirical median profile, the resulting MF would be a factor of 2 higher. In Fig. 2, we also plot a power-law form with index 1.3, proportional to the median truncated-to-original mass ratio profile in the HCFJ model.

Once the $\mu(r)$ profile has been determined, defining $1 + f_{rel}(r, M_s^{tr})$ as $\mathcal{N}^{stp}(r, M_s^{tr})/\mathcal{N}^{tr}(r, M_s^{tr})$, equation (18) can be rewritten in the form

$$\mathcal{N}^{stp}\left(r, M_s^{tr}\right) = [1 + f_{rel}(r)]\,\mu(r)\,\mathcal{N}^{acc}\left(r, M_s^{tr}\right), \quad (22)$$

where $f_{rel}(r)$ is the proportion of stripped subhaloes previously locked as subsubhaloes within accreted subhaloes per each stripped subhalo directly arising from the truncation of an accreted subhalo. That proportion is the solution of the Fredholm integral equation of second kind that follows from equation (18) (see Appendix A),

$$1 + f_{rel}(r) = 1 + 3\,\frac{r^3}{R_h^3}\,\int_0^{R_h} dr'\, r'^2\, F(r', r)$$

$$\times\,[1 + f_{rel}(r')]\frac{\mu(r')}{\mu(r)}\frac{\rho(r')}{\bar{\rho}(R_h)}, \quad (23)$$

where $F(r', r)$ is the cumulative velocity distribution function (see Appendix C for the corresponding differential form) for the velocity v such that $Q_{v(v,r)}(v, r) = r'$, where $Q_{v(v,r)}(v, r)$ is the ratio of truncated-to-original subhalo radii after $v(v, r)$ passages by pericentre calculated in Section 3. As shown in Fig. 3, the fraction $f_{rel}(r)$ increases with increasing radius and reaches a maximum value of 0.06 in current haloes. We remark that even though the contribution of subsubhaloes to the properties of substructure has been included in previous analytic models (e.g. Taylor & Babul 2004; Zentner et al. 2005) and simulations (e.g. Han et al. 2012, 2018), a quantitative estimate of the contribution of released subsubhaloes as that given here was missing.

Note that $f_{rel}(r)$ depends on disruption through $F(r', r)$. Yet, like in the case of $\mu(r)$, we have found no significant difference down to one thousandth R_h between null and moderate disruption. Thus, disruption does not affect the predicted abundance of stripped subhaloes, $\mathcal{N}^{stp}(r, M_s^{tr})$, which supports the claim by van den Bosch et al. (2018) that it is likely a numerical effect (see also Errani & Peñarrubia 2020).

Equation (22) states that the abundance of stripped subhaloes is proportional to the abundance of accreted subhaloes with propor-
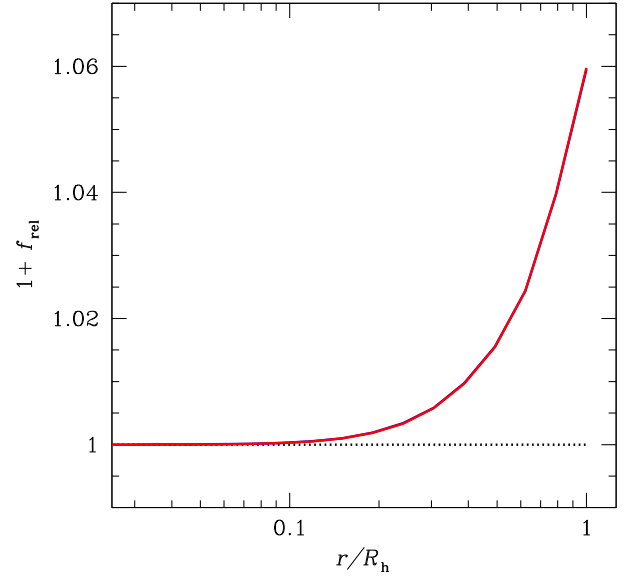

Figure 3. Function $f_{rel}(r)$ predicted for MW-mass haloes. At the scale of the figure, the solutions corresponding to a SWV-like simulation and a real 100 GeV WIMP universe overlap.

tionality factor equal to $[1 + f_{rel}(r)]\mu(r)$. This resembles the relation found in the HCFJ model with the median truncated-to-original subhalo mass ratio playing the role of $\mu(r)$. We remark, however, that the relation with the mean truncated-to-original subhalo mass ratio profile is essentially exact (see equation 21, but see Section 6), while the equivalent one in the HCFJ model is a relation between typical quantities holding for subhaloes.

From equations (22) and (20) we see that $\mathcal{N}^{stp}(r, M_s^{tr})$ is separable like $\mathcal{N}^{acc}(r, M_s^{tr})$. This is the reason that the mean number density profile per infinitesimal mass of stripped subhaloes, $n^{stp}(r, M_s^{tr}) \equiv \mathcal{N}^{stp}(r, M_s^{tr})/(4\pi r^2)$, scaled to the mean number density per infinitesimal mass of such subhaloes, $\bar{n}^{stp}(R_h, M_s^{tr}) \equiv 3\mathcal{N}^{stp}(M_s^{tr})/(4\pi R_h^3)$, takes the mass-independent form (see equations 20–22)

$$\frac{n^{stp}\left(r, M_s^{tr}\right)}{\bar{n}^{stp}\left(R_h, M_s^{tr}\right)} = \frac{[1 + f_{rel}(r)]\mu(r)}{(1 + f_{rel})\mu(R_h)}\frac{\rho(r)}{\bar{\rho}(R_h)}. \quad (24)$$

Thus the scaled number density profiles of stripped subhaloes of different truncated masses M_s^{tr} overlap in one single profile (but see Section 6), as found in Paper I for accreted subhaloes and in agreement with the results of SWV (see also Ludlow et al. 2009). However, contrarily to what happens with the profile of accreted subhaloes that of stripped subhaloes is not proportional to $\rho(r)$ but bends downwards at small radii (Fig. 4) also in agreement with the results of simulations (Ghigna et al. 1998; Diemand, Moore & Stadel 2004; Gao et al. 2004; Nagai & Kravtsov 2005; Diemand et al. 2007; SWV). Equation (22) shows that such a bending is due to the factor $\mu(r)$, which, as we will see in Section 5, entails an increasing abundance of dDM towards the halo centre. More importantly, the predicted profile recovers that found in the Aquarius halo A regardless of the exact form of $\mu(r)$ below $r = 0.08R_h$, showing that the agreement between our prediction for purely accreting haloes and the properties of the halo A is compelling regardless of the growth of the halo before $z = 6$. We thus find the same result as the HCFJ model using the median truncated-to-original subhalo mass ratio profile instead of the mean one. This could be foreseen since
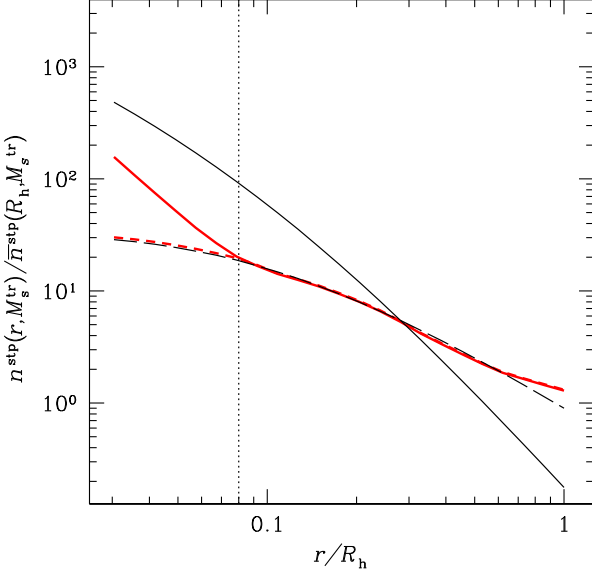
Figure 4. Scaled number density profiles for stripped subhaloes of different masses and similar concentrations predicted for purely accreting MW-mass haloes from the two versions of the $\mu(r)$ profiles obtained using the Gao et al. (2008) *M–c* relation shown in Fig. 3 (same lines). For comparison we plot the profile of the form $\propto r^{1.3}\rho(r)$ (long-dashed black line) providing a good fit to the scaled subhalo density profile of the Level 1 Aquarius halo A (HCFJ) and the scaled mass density profile $\rho(r)$ of that halo (solid black line). The vertical dotted line marks the radius out of which the halo A has evolved by accretion as considered in CUSP.

any constant shift between the two profiles cancels when deriving the 'scaled' density profile.

Integrating over r the abundance of stripped subhaloes given in equation (22), we obtain the differential MF of stripped subhaloes per infinitesimal mass,

$$\mathcal{N}^{\mathrm{stp}}\left(M_{\mathrm{s}}^{\mathrm{tr}}\right) = \overline{(1 + f_{\mathrm{rel}})\mu}(R_{\mathrm{h}})\,\mathcal{N}^{\mathrm{acc}}\left(M_{\mathrm{s}}^{\mathrm{tr}}\right). \quad (25)$$

According to this relation, $\mathcal{N}^{\mathrm{stp}}(> M_{\mathrm{s}}^{\mathrm{tr}})$ is proportional to $\mathcal{N}^{\mathrm{acc}}(> M_{\mathrm{s}}^{\mathrm{tr}})$, which agrees with the results of simulations (HCFJ) at least at intermediate and low masses (see below). As shown in Fig. 5, the corresponding cumulative MF is in fairly good agreement with that found in simulations. Specifically, at low masses it is approximately a power-law form with a logarithmic slope of ~ -0.95 (the logarithmic slope of the MF of accreted subhaloes varies from -0.94 to -0.97 from high to low subhalo masses; Paper I), which is intermediate between the slopes of -0.9 and -1 reported by SWV and Diemand et al. (2007), respectively, and very close to -0.94 (Boylan-Kolchin et al. 2010; Gao et al. 2011) and -0.95 at $M_{\mathrm{s}}/M_{\mathrm{h}} \sim 10^{-5}$ (HCFJ; Han et al. 2018).

5 ABUNDANCE AND RADIAL DISTRIBUTION OF DIFFUSE DARK MATTER

The total mass density of the halo at r results from the contribution of stripped subhaloes and dDM. We thus have that the total dDM mass fraction $f_{\mathrm{dDM}}^{\mathrm{stp}}(r)$ at r satisfies

$$\left[1 - f_{\mathrm{dDM}}^{\mathrm{stp}}(r)\right]\rho(r) = \frac{1}{4\pi r^2}\int_{M_{\mathrm{min}}}^{M_{\mathrm{h}}}\mathrm{d}M_{\mathrm{s}}^{\mathrm{tr}}\,M_{\mathrm{s}}^{\mathrm{tr}}\,\mathcal{N}^{\mathrm{stp}}\left(r, M_{\mathrm{s}}^{\mathrm{tr}}\right), \quad (26)$$

where M_{min} is the minimum halo mass at the origin of dDM (see Paper I). Taking into account equations (22) and (20), equation (26)
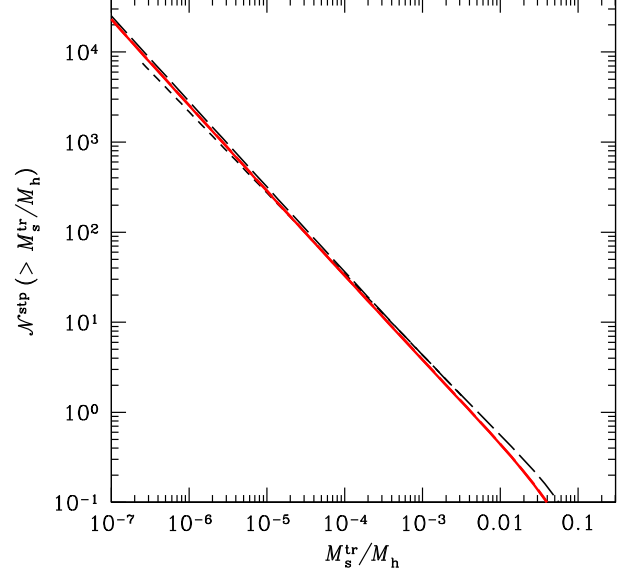

Figure 5. Cumulative MF of stripped subhaloes predicted in purely accreting MW-mass haloes from the mean $\mu(r)$ profile (solid red line) and its extrapolation to $r < 0.08R_{\mathrm{h}}$ (dashed red line) compared to the MF of the Level 1 Aquarius halo A obtained by SWV (short-dashed black line) and the general MF for haloes of that mass found by Han et al. (2018) (long-dashed black line).
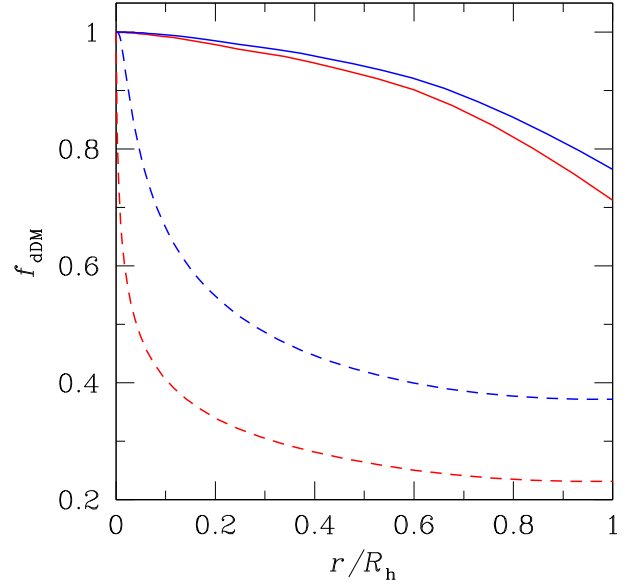

Figure 6. Total (accreted plus stripped) dDM mass fraction profiles in purely accreting MW-mass haloes predicted in a real 100 GeV WIMP universe (solid red line) and a SWV-like simulations (solid blue line). Dashed lines give the corresponding accreted dDM mass fraction profiles derived in Paper I.

leads to

$$1 - f_{\mathrm{dDM}}^{\mathrm{stp}}(r) = [1 + f_{\mathrm{rel}}(r)]\,\mu(r)\left[1 - f_{\mathrm{dDM}}^{\mathrm{acc}}(r)\right]. \quad (27)$$

In Fig. 6, we plot the total dDM mass fraction profile $f_{\mathrm{dDM}}^{\mathrm{stp}}(r)$ for purely accreting MW-mass haloes (equation 27) for the same illustrative cases as used in Paper I to calculate the accreted dDM mass fraction at r, $f_{\mathrm{dDM}}^{\mathrm{acc}}(r)$ (also plotted in Fig. 6): (1) a real 100 GeV

WIMP universe with minimum halo mass $M_{min} = 10^{-6}$ M$_\odot$ and t_{min} equal to the time of decoupling; and (2) a SWV-like simulation starting at $t_{min} = 0.0124$ Gyr ($z_{min} = 127$) and with a resolution mass of $M_{min} = 4.4 \times 10^5$ M$_\odot$. As can be seen, the dDM mass fraction in current haloes is quite large; it is still ~ 0.75 at R_h where it reaches the minimum value. Moreover, a substantial fraction has been stripped from subhaloes. Specifically, in the 100 GeV WIMP universe, we find that 92 per cent of the total mass of MW-like haloes is in the form of dDM, with 33 per cent directly accreted from the intrahalo medium (Paper I; see also Angulo & White 2010). And in SWV-like simulations, 95 per cent of the total mass of those haloes is typically in the form of dDM, with 51 per cent directly accreted (Paper I; see also Wang et al. 2011).

The relation (27) allows one to rewrite the scaled subhalo number density of stripped subhaloes (24) in the form

$$\frac{n^{stp}\left(r, M_s^{tr}\right)}{\bar{n}^{stp}\left(R_h, M_s^{tr}\right)} = \frac{f_s(r)}{\bar{f}_s(R_h)} \frac{\rho(r)}{\bar{\rho}(R_h)}, \qquad (28)$$

where $f_s(r)$ is the stripped to accreted subhalo mass ratio profile, equal to $[1 - f_{dDM}^{stp}(r)]/[1 - f_{dDM}^{acc}(r)]$. Comparing expressions (28) and (24), we see that the bending of the scaled number density profile of stripped subhaloes with respect to the scaled density profile of the host halo found in simulations, shown to obey the factor $[1 + f_{rel}(r)]\mu(r)$, can also be seen to obey the factor $[1 - f_{dDM}^{stp}(r)]/[1 - f_{dDM}^{acc}(r)]$. Thus, such a bending is due to the increasing abundance of dDM mass towards the halo centre due to the stripping of subhaloes (SWV; Angulo et al. 2009; Gao et al. 2012; Hellwing et al. 2016; Fielder et al. 2020). Likewise, taking into account the relation (27), the MF of stripped subhaloes, equation (25), can be rewritten in the form

$$\mathcal{N}^{stp}\left(M_s^{tr}\right) = \bar{f}_s(R_h)\mathcal{N}^{acc}\left(M_s^{tr}\right). \qquad (29)$$

6 THE EFFECT OF THE MASS-DEPENDENT CONCENTRATIONS

In Sections 4 and 5, we have taken into account that subhaloes accreted at different times $t(r)$ have different typical concentrations. But halo concentration also slightly depends on their mass. In this section we explicitly account for this latter dependence.

A first important consequence of such a dependence is that, according to the results of Section 3, the HCJF condition 3 would be only approximate. This is not contradictory with the results of simulations. That condition, which followed from the HCFJ stripping model where subhaloes were approximated by isothermal spheres with mass-independent density profiles, was shown by these authors to be consistent with the results of simulations but not confirmed by them. Certainly it was shown to lead to a mass-independent scaled number density profile of stripped subhaloes as found in simulations (e.g. SWV; Ludlow et al. 2009). But this latter result has also been shown to be only approximate. The more detailed study carried by Han et al. (2018) has found, indeed, that the scaled number density profile of subhaloes actually depends on their mass (see the discussion below). On the other hand, as shown next, our stripping model in its more accurate version taking into account the mass dependence of halo concentration also leads to the same approximate result, so we must not worry about the idea that the HCFJ condition 3 is approximate just as our previous results.

Having said this, we can follow essentially the same steps as in Section 4 using the full time and mass dependence encoded in the M–c relation. Of course, if we are to recover the radial abundance and MF of stripped subhaloes observed in simulated haloes, we should use
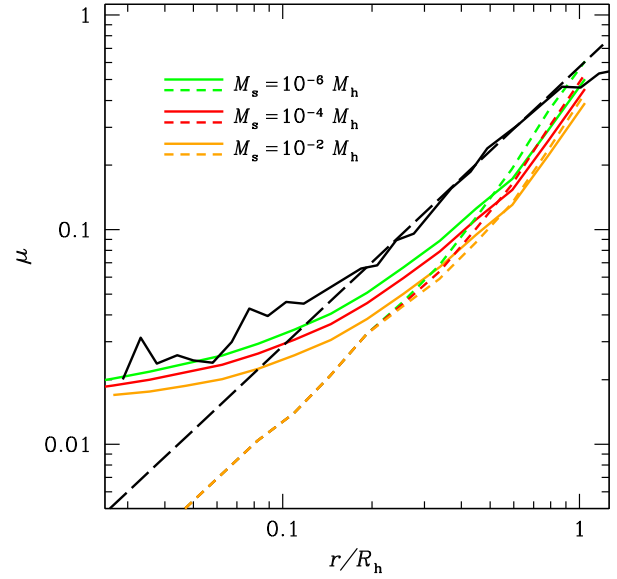

Figure 7. Mean truncated-to-original subhalo mass ratio profile predicted in purely accreting MW-mass haloes for different subhalo masses (coloured lines) from the respective $\mu(r, M_s)$ profiles obtained using the CUSP M–c relation (solid lines) and the extrapolated $\mu(r, M_s)$ profiles obtained from the Gao et al. (2008) M–c relation (dashed lines). As references, we also plot the empirical median truncated-to-original subhalo mass ratio profile found by HCFJ in the Level 1 Aquarius halo A (solid black line) and its modelled version (long-dashed black line), both depicted in Fig. 4.

the empirical M–c relation found by e.g. Gao et al. (2008) affected by the limited mass resolution of simulations giving rise to those empirical properties as done in Section 4. But we are also interested in deriving the real (unbiased) radial abundance and MF of stripped subhaloes predicted by CUSP, so we will use, in addition, the M–c relation directly arising from our formalism (see Salvador-Solé et al., in preparation) and see the differences in the results obtained from both M–c relations.

In Fig. 7, we show the μ profiles obtained for several subhalo masses. At large r the solutions arising from the two M–c relations are very similar. This is not unsurprising since both relations behave very similarly at low-z. Specifically, the solutions obtained for different subhalo masses are more or less shifted vertically as expected, though the amplitude of those shifts slightly depend on the particular M–c relation used due to their slightly different shape.[7] At $r \lesssim 0.2R_h$, however, the solutions drawn from the two M–c relations deviate from each other. In the case of the empirical relation, the (extrapolated) curves for different masses converge at $r < 0.02R_h$ and are kept with the same power-law shape as at larger radii. (The reason for their convergence is that the log–log M–c relation provided by Gao et al. becomes a horizontal line at z somewhat higher than 3, meaning that all subhaloes with different masses have identical concentrations there.) While, in the case of the theoretical M–c relation, the curves for the different subhalo masses show the same vertical shifts as at large r but deviate from a power law of index ~ 1.3 and become increasingly less steep towards the centre.

---

[7]At $z = 0$, Gao et al. (2008) M–c relation is linear in log–log, while that predicted by CUSP becomes slight shallower towards small masses.
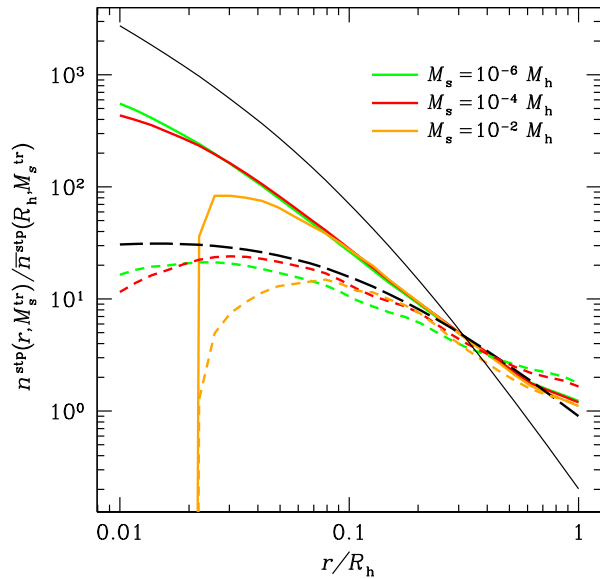
Figure 8. Scaled number density profiles of stripped subhaloes of different masses (coloured lines) predicted for purely accreting haloes using the M–c relation found in simulations by Gao et al. (2008) (dashed lines) and the theoretical M–c relation predicted by CUSP (solid lines). The long-dashed black line is the HCFJ fit to the profile found for low enough mass subhaloes in the Level 1 Aquarius halo A. The solid black line is the scaled halo density profile. All empirical data have been converted to M_h.

A good approximation for those μ profiles, particularly for the case of the CUSP M–c relation, is thus

$$\mu_{[M_h, t_h]}(r, M_s) \approx \mu_{[M_h, t_h]}(r, M_{s0})\, G(M_s),\qquad(30)$$

with M_{s0} an arbitrary mass and $G(M_s)$ equal to $(M_s/M_{s0})^\alpha$ with $\alpha \approx -0.03$ in the case of the CUSP M–c relation and the same expression at $r \geq 0.2R_h$ (otherwise with no dependence on M_s) in the case of Gao et al.'s M–c relation. Note that the concentration of the host halo at $t(r)$ is not the typical concentration of haloes at that time but r/r_s so that decreasing M_s by some factor and keeping M_h fixed is not equivalent to keeping M_s fixed and increasing M_h by the same factor. Consequently, $\mu_{[M_h, t_h]}(r, M_s)$ is not a power law of M_h with index $-\alpha$.

Then, the same derivation leading from equation (19) to equation (21) leads to

$$\mathcal{N}^{stp}_{[M_h, t_h]}\left(r, M_s^{tr}\right) = g(\alpha)\left[1 + f_{rel}\left(r, M_s^{tr}\right)\right] \mu_{[M_h, t_h]}\left(r, M_s^{tr}\right)$$
$$\times\, \mathcal{N}^{acc}_{[M_h, t_h]}\left(r, M_s^{tr}\right),\qquad(31)$$

with the factor $g(\alpha)$ equal to 1 or $1 - \alpha$ depending on whether $G(M_s)$ in equation (30) is unity or not. Note that the function f_{rel} solution of the differential equation (23) for the function $\mu_{[M_h, t_h]}(r, M_s^{tr})$ also depends now on M_s^{tr}.

The resulting scaled number density profiles of stripped subhaloes of different masses obtained from direct calculation not using the approximation (30) are shown in Fig. 8. In the case of the empirical M–c relation they are relatively close to the empirical profile of the Aquarius halo A found by SWV and HCFJ, except for the fact that they do not exactly overlap with each other owing to the fact that the vertical shifts in the corresponding μ profiles are not constant over all radii. On the contrary, the constant vertical shifts found in the case of the theoretical M–c relation go unnoticed in the scaled number density profiles of stripped subhaloes of different masses,
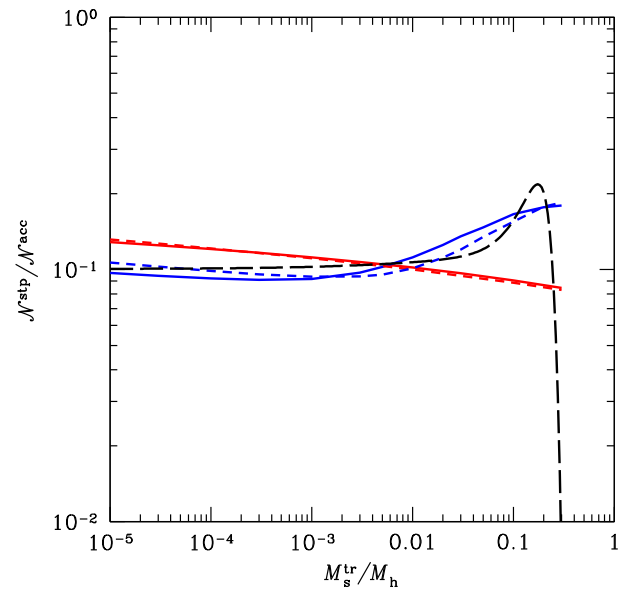

Figure 9. Ratio of the differential MFs of stripped and accreted subhaloes predicted for haloes of different masses (with the appropriate scaling; see text) obtained using the Gao et al. (2008) and CUSP M–c relations (dashed and solid lines, respectively) compared to the ratio found in simulations by Han et al. (2018) (long-dashed black line), both of them scaled with halo mass as explained in the text. The two solutions depicted are those obtained from the stripping model of Section 3 but accounting for the mass-dependent subhalo concentration (red lines) and the same model with suppression of stripping when the mass of subhaloes is larger than $M(r_{per})$ (blue lines).

which thus overlap. Strictly speaking the profiles for different M_s show different cut-offs, which simply reflects that no subhalo with a given mass M_s can be accreted by the halo of mass $M(r) < 3M_s$ as this would cause a major merger with the destruction of the subhalo (see Paper I). However, the resulting number density profile is in this case less bent with respect to the $\rho(r)$ profile at small radii than in the Aquarius halo A. This disagreement does not mean, of course, that the theoretical prediction is wrong. Rather the contrary, what would be biased is the empirical profile due to the limited mass resolution of simulations affecting the M–c relation. Our prediction suffers, instead, from the fact that, in its current version, our stripping model does not include the effects of dynamical friction that are particularly strong at the subhalo high-mass end (see below).

Even though the scaled number density of subhaloes of different masses nearly overlaps, the non-scaled ones do not because of the different total number of subhaloes of different masses. In fact, the detailed, non-scaled and scaled, number density profiles of massive stripped subhaloes are found to be cuspier than those of less massive subhaloes (Han et al. 2018). As discussed by these authors, this result seems to be the consequence of dynamical friction, which causes massive subhaloes to migrate towards the centre of the host halo. In fact, dynamical friction would not only alter the 'natural' density profiles of stripped subhaloes but also their MF. Indeed, even though the MF does not depend on the radial location of subhaloes, it appears that dynamical friction also affects the stripping itself of massive subhaloes and, hence, the MF of stripped subhaloes, too.

In Fig. 9, we depict the ratio between the differential MFs of stripped and accreted subhaloes as function of the scaled mass $m = M_s^{tr}/M_h$ that result from integration over r of the relation (31) with the μ profiles obtained from the two different M–c

relations. The ratios for different halo masses have been multiplied by $\bar{\mu}_{[M_{h0},t_h]}(R_{h0}, M_{s0})/\bar{\mu}_{[M_h,t_h]}(R_h, M_{s0})$, where M_{h0} is an arbitrary halo mass and R_{h0} its corresponding virial radius so that the curves for different halo masses overlap (see equations 30 and 31, with f_{rel} neglected in front of unity). That scaling factor turns out to behave as $(M_h/M_{h0})^\eta$ with $\eta = -0.09$ and -0.08 in the Gao et al. (2008) and CUSP M–c relations, respectively. For comparison, we also plot the ratio found for different halo masses by Han et al. (2018) multiplied by the factor $(M_h/M_{h0})^{-0.1}$, which also causes those empirical curves to overlap (Rodríguez-Puebla et al. 2016; Han et al. 2018). Note that the empirical MF of stripped subhaloes plotted in this figure is not normalized as the original MF in Han et al. (2018). The reason for this is that the latter holds for subhaloes of all levels, while we are interested in the MF of first-level subhaloes only. We have thus shifted it downwards keeping the same proportion with respect to the MF of accreted subhaloes correctly renormalized so as to hold for first-level subhaloes only (see Paper I). Even though that empirical MF of stripped subhaloes is more comparable to the predicted MF, we cannot guarantee yet that its normalization is fully correct.

The theoretical ratios derived from both M–c relations substantially deviate from the empirical one. While the former decreases slowly with increasing m, the latter increases, shows a marked bump, and rapidly falls to zero at the high-mass end (Jiang & van den Bosch 2016; Han et al. 2018). This disagreement is due to the fact that our stripping model fails for massive subhaloes. Indeed, as pointed out by Han et al. (2018), the tidal force from the host halo on very massive subhaloes becomes less important than its self-gravity, so stripping is less effective. Properly accounting for that effect is out of scope of this paper because our model does not include dynamical friction, while that effect alters the pericentre of subhaloes and, hence, the mass of the host halo seen by subhaloes there, $M[r_{per}(r, v)]$. To see the kind of effect this condition may have we depict in Fig. 9 the result of suppressing stripping when the geometrical mean of M_s and $M_s^{tr}(v, r, M_s)$ is more massive than $M[r_{per}(r, v)]$.[8] As can be seen, the trend of the new MF (normalized as the empirical one) greatly improves, indeed.

However this effect increases the ratio towards high masses, which goes in the opposite direction from that needed to find the exponential cut-off at the high-mass end of the empirical ratio. That cut-off is likely due, once again, to the effects of dynamical friction. Indeed, extremely massive subhaloes rapidly migrate to the halo centre and merge with the central subhalo, so they 'disappear' rather than stay a little less stripped. Of course, even without that effect, the predicted differential MFs of stripped subhaloes end up by falling off to zero as M_s^{tr} approaches $M_h/3$ due to the similar cut-off present in the differential MF of accreted subhaloes (see Paper I).

We thus see that accounting for the mass dependence of halo concentration is not enough to reproduce the detailed differential MF of stripped subhaloes. To do that we need, in addition, to include the effects of dynamical friction. Nevertheless, our model finds the dependence on halo mass of the MF of stripped subhaloes (the MF of accreted subhaloes is universal; see Paper I). This result, which is the direct consequence of the dependence of stripping on halo concentration, is very robust as it is little sensitive to the particular M–c relation adopted. This success thus gives strong support to the central role of halo concentration in subhalo stripping as considered in our model (see also Chua et al. 2017). This would be the origin of
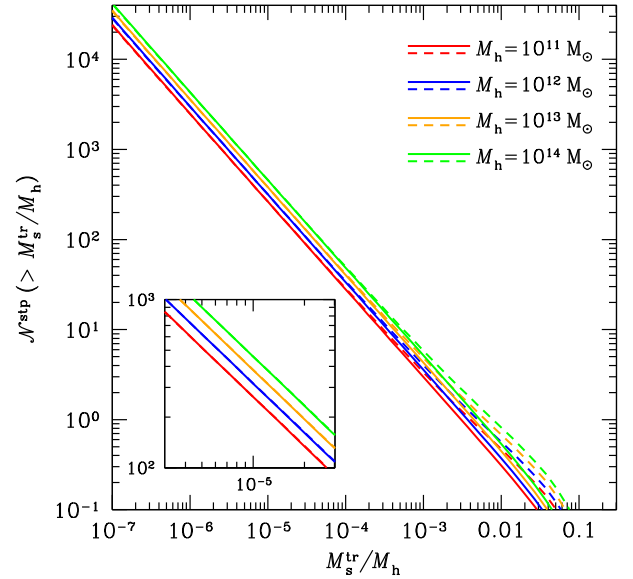

Figure 10. Cumulative MF of stripped subhaloes predicted for several halo masses (coloured lines). We plot the results obtained from our original stripping model with mass-dependent subhalo concentrations according to the Gao et al. (2008) M–c relation (solid lines) and the corrected and renormalized version with suppression of stripping when the mass of subhaloes is larger than $M(r_{per})$ (dashed lines).

the mass dependence of the cumulative MFs of stripped subhaloes (see Fig. 10) found in simulations (Zentner et al. 2005; Giocoli et al. 2008; Gao et al. 2011; Ishiyama et al. 2021).

7 SUMMARY AND DISCUSSION

Using the results of Paper I on accreted subhaloes and dDM, we have calculated the typical (mean) abundance and radial distribution of stripped subhaloes and dDM in current MW-mass haloes in a ΛCDM cosmology. To do this we have modelled the repetitive tidal stripping and heating suffered by subhaloes orbiting within purely accreting host haloes ignoring the effects of dynamical friction.

Contrarily to the derivation followed in Paper I, which was achieved from first principles and with no single free parameter, that followed here has involved a model of subhalo tidal heating with two free parameters. We remark, however, that these parameters have not been tuned to get a good fit to the final properties of substructure found in simulations, but just to fit the effect of repetitive stripping and heating found in dedicated numerical experiments. As the general conclusions reached do not depend on the particular values of these parameters, we can thus still say that the derivation followed is parameter free.

Our detailed treatment has paid special attention to the role of the dDM and subhaloes previously locked within accreted subhaloes and released in the intrahalo medium through the stripped material. The proportion of stripped subhaloes arising from released subsubhaloes per each accreted subhalo is only of 6 per cent at the outer radius where it reaches the maximum value in current MW-mass haloes. Thus, this contribution to the total abundance of stripped subhaloes can be neglected in a first approximation. In respect to the proportion of released to accreted dDM, it starts increasing with increasing halo radius at $r \sim 2 \times 10^{-4} R_h$ ($12 \times 10^{-3} R_h$), reaches a maximum of about 3 (1.7) at $r \sim 0.1 R_h$ ($0.1 R_h$), and then decreases until a value of 2 (1) at the virial radius of current MW-mass haloes in a real 100

---

[8]That geometrical mean increases the mass of the stripped subhalo so as to compensate that the real r_{per} is smaller than calculated without dynamical friction.

GeV WIMP universe (and a SWV-like simulation). This represents a total dDM mass fraction of ∼0.95 in both cases. In other words, the structure of current haloes is amply dominated, particularly in the central region, by dDM, which has important consequences for the boost factor of the theoretical DM annihilation signal.

We have clarified the origin of HCFJ conditions shown to encode the properties of substructure. In Paper I, the conditions 1 and 2 were demonstrated to arise directly from the properties of peaks in the Gaussian random field of density perturbations. In this paper, we have shown that condition 3 stating that the truncated-to-original subhalo mass ratio profile does not depend on subhalo mass arises from the similar concentrations of accreted subhaloes, together with the fact that subhaloes suffer maximum tidal stripping at pericentre, where they are truncated at the radius encompassing a mean inner density of the order of that of the host halo there. However, according to our results, HCFJ condition 3 is only approximate because of the weak but non-negligible dependence of subhalo concentration on mass. None the less, this dependence has little effect on the scaled subhalo number density profile, which is kept essentially independent of subhalo mass as found in simulations (provided dynamical friction is ignored; Han et al. 2018).

Given the dependence of subhalo concentration on mass, our detailed quantitative results depend on the exact M–c relation assumed. When we use the empirical M–c relation found in simulations by Gao et al. (2008), our predicted scaled number density profile of stripped subhaloes fully reproduces the empirical one found by HCFJ in the Aquarius simulation halo A, which is substantially shallower than the density profile of the host halo. This is so despite that the predicted mean truncated-to-original subhalo mass ratio is substantially lower than the corresponding empirical median profile derived by HCFJ. This result, which is contrary to the expectations for the lognormal distribution of truncated-to-original mass ratios, is likely due to the fact that the median profile obtained by HCFJ has been derived for subhaloes of all levels, while our predictions are for first-level ones only. Since the number of subhaloes of any mass at all levels is twice that of first-level subhaloes (Paper I), the only ones undergoing stripping, it is not surprising that the truncated-to-original profile for subhaloes of the former population is notably higher than for the latter one, while they both have the same *scaled* number density profile. When the unbiased M–c relation predicted by CUSP is used, the predicted mean truncated-to-original subhalo mass ratio somewhat changes, but the general trend is similar. In particular, the corresponding scaled number density profile becomes substantially steeper, but it is also kept less steep than the mass density profile of the halo. This robust result is the consequence of the higher concentration of dDM towards the halo centre. On the other hand, the predicted subhalo MF reproduces the subhalo MF and its dependence on halo mass found in simulations, regardless of the particular M–c relation used.

All these results have been derived neglecting the effects of dynamical friction. This is an important limitation for stripped subhaloes with masses above $10^{-4}M_h$, whose radial distribution and MF are notably affected by that mechanism. This is the reason why we are currently working in the implementation of an accurate analytic treatment of dynamical friction in the stripping model.

On the other hand, the results presented hold for haloes having grown by pure accretion. As shown in Salvador-Solé & Manrique (2021), the violent relaxation that takes place in major mergers causes the system to lose the memory of its past assembly history, so the general properties inferred for purely accreting haloes also hold for ordinary haloes having suffered major mergers. However, that general rule does not hold for stripped subhaloes because the imprints of stripping are not erased by violent relaxation. Thus, even though the results found here for purely accreting haloes reproduce the properties of substructure found in the Level 1 Aquarius halo A having been accreting since $r \sim 0.08R_h$ and also seem to agree with the properties of substructure found in simulated haloes in general, we cannot discard that such properties slightly depend on the merger history of haloes. The more realistic case of haloes having suffered major mergers is addressed in Paper III, where we focus on very low mass subhaloes whose properties should not be influenced by dynamical friction.

DATA AVAILABILITY

The data underlying this paper will be shared on reasonable request to the corresponding author.

REFERENCES

Angulo R. E., Lacey C. G., Baugh C. M., Frenk C. S., 2009, MNRAS, 399, 983

Angulo R. E., White S. D. M., 2010, MNRAS, 401, 1796

Bardeen J. M., Bond J. R., Kaiser N., Szalay A. S., 1986, ApJ, 304, 15

Benson A. J. et al., 2013, MNRAS, 428, 1774

Binney J., Tremaine S., 2008, Galactic Dynamics, 2nd edn. Princeton Univ. Press, Princeton, NJ

Bose S., Deason A. J., Belokurov V., Frenk C. S., 2020, MNRAS, 495, 743

Bose S., Hellwing W. A., Frenk C. S., Jenkins A., Lovell M. R., Helly J. C., Li B., 2016, MNRAS, 455, 318

Boylan-Kolchin M., Springel V., White S. D. M., Jenkins A., 2010, MNRAS, 406, 896

Bryan G. L., Norman M. L., 1998, ApJ, 495, 80

Cautun M., Hellwing W. A., van de Weygaert R., Frenk C. S., Jones B. J. T., Sawala W., 2014, MNRAS, 445, 2049

Chua K. T. E., Pillepich A., Rodriguez-Gomez V., Vogelsberger M., Bird S., Hernquist L., 2017, MNRAS, 472, 4343

Cole S., Lacey C., 1996, MNRAS, 281, 716

Diemand J., Kuhlen M., Madau P., 2007, ApJ, 657, 267

Diemand J., Moore B., Stadel J., 2004, MNRAS, 353, 624

Einasto J., 1965, Trudy Inst. Astrofiz. Alma-Ata, 5, 87

Elahi P. J., Widrow L. M., Thacker R. J., 2009, Phys. Rev. D, 80, 123513

Errani R., Peñarrubia J., 2020, MNRAS, 491, 4591

Fielder C. E., Mao Y.-Y., Zentner A. R., Newman J. A., Wu H.-Y., Wechsler R. H., 2020, MNRAS, 499, 2426

Font A. S. et al., 2020, MNRAS, 498, 1765

Font A. S., McCarthy I. G., Belokurov V., 2021, MNRAS, 505, 783

Fujita Y., Sarazin C. L., Nagashima M., Yano T., 2002, ApJ, 577, 11

Gao L., Frenk C. S., Boylan-Kolchin M., Jenkins A., Springel V., White S. D. M., 2011, MNRAS, 410, 2309

Gao L., Frenk C. S., Jenkins A., Springel V., White S. D. M., 2012, MNRAS, 419, 1721

Gao L., Navarro J. F., Cole S., Frenk C. S., White S. D. M., Springel V., Jenkins A., Neto A. F., 2008, MNRAS, 387, 536

Gao L., White S. D. M., Jenkins A., Stoehr F., Springel V., 2004, MNRAS, 355, 819

Ghigna S., Moore B., Governato F., Lake G., Quinn T., Stadel J., 1998, MNRAS, 300, 146

Giocoli C., Tormen G., Sheth R. K., van den Bosch F. C., 2010, MNRAS, 404, 502

Giocoli C., Tormen G., van den Bosch F. C., 2008, MNRAS, 386, 2135

Gnedin O. Y., Ostriker J. P., 1999, ApJ, 513, 626

González-Casado G., Mamon G. A., Salvador-Solé E., 1994, ApJ, 433, L61

Green S. B., van den Bosch F. C., 2019, MNRAS, 490, 2091

Griffen B. F., Ji A. P., Dooley G. A., Gómez F. A., Vogelsberger M., O'Shea B. W., Frebel A., 2016, ApJ, 818, 10

Han J., Cole S., Frenk C. S., Benitez-Llambay A., Helly J., 2018, MNRAS, 474, 604

Han J., Cole S., Frenk C. S., Jing Y., 2016, MNRAS, 457, 1208 (HCFJ)

Han J., Jing Y. P., Wang H., Wang W., 2012, MNRAS, 427, 2437

Hansen S. H., Moore B., Zemp M., Stadel J., 2006, J. Cosmol. Astropart. Phys., 01, 014

Hayashi E., Navarro J. F., Taylor J. E., Stadel J., Quinn T., 2003, ApJ, 584, 541

Hellwing W. A., Frenk C. S., Cautun M., Bose S., Helly J., Jenkins A., Sawala T., Cytowski M., 2016, MNRAS, 457, 3492

Henry J. P., 2000, ApJ, 534, 565

Ishiyama T. et al., 2021, MNRAS, 506, 4210

Jiang F., Dekel A., Freundlich J., van den Bosch F. C., Green S. B., Hopkins P. F., Benson A., Du X., 2021, MNRAS, 502, 621

Jiang F., van den Bosch F. C., 2016, MNRAS, 458, 2848

Jiang L., Cole S., Sawala T., Frenk C. S., 2015, MNRAS, 448, 1674

Juan E., Salvador-Solé E., Domènec G., Manrique A., 2014a, MNRAS, 439, 719

Juan E., Salvador-Solé E., Domènech G., Manrique A., 2014b, MNRAS, 439, 3156

Kampakoglou M., Benson A. J., 2007, MNRAS, 374, 775

King I., 1962, AJ, 67, 471

Klypin A. A., Trujillo-Gomez S., Primack J., 2011, ApJ, 740, 102

Klypin A., Gottöber S., Kravtsov A. V., 1999, ApJ, 516, 530

Komatsu E. et al., 2011, ApJS, 192, 18

Lee J., 2004, ApJ, 604, L73

Lovell M. R., Frenk C. S., Eke V. R., Jenkins A., Gao L., Theuns T., 2014, MNRAS, 439, 300

Ludlow A. D., Navarro J. F., Springel V., Jenkins A., Frenk C. S., Helmi A., 2009, ApJ, 692, 931

Manrique A., Raig A., Solanes J. M., González-Casado G., Stein P., Salvador-Solé E., 1998, ApJ, 499, 548

Manrique A., Salvador-Solé E., 1995, ApJ, 453, 6

Manrique A., Salvador-Solé E., 1996, ApJ, 467, 504

Mo H., van den Bosch F. C., White S., 2010, Galaxy Formation and Evolution. Cambridge Univ. Press, Cambridge

Nagai D., Kravtsov A. V., 2005, ApJ, 618, 557

Navarro J. F., Frenk C. S., White S. D. M., 1997, ApJ, 490, 493

Oguri M., Lee J., 2004, MNRAS, 355, 120

Onions J. et al., 2012, MNRAS, 423, 1200

Peñarrubia J., Benson A. J., 2005, MNRAS, 364, 977

Peñarrubia J., Navarro J. F., McConnachie A. W., 2008, ApJ, 673, 226

Pullen A. R., Benson A. J., Moustakas L. A., 2014, ApJ, 792, 24

Read J. L., Wilkinson M. I., Evans N. W., Gilmore G., Kleyna J. T., 2006, MNRAS, 366, 429

Richings J. et al., 2020, MNRAS, 492, 5780

Rodríguez-Puebla A., Behroozi P., Primack J., Klypin A., Lee C., Hellinger D., 2016, MNRAS, 462, 893

Salvador E., Manrique A., Canales D., Botella I., 2021, MNRAS, submitted to MNRAS (Paper III)

Salvador-Solé E., Manrique A., 2021, ApJ, 914, 141

Salvador-Solé E., Manrique A., Botella I., 2021, MNRAS, in press (Paper I)

Salvador-Solé E., Serra S., Manrique A., González-Casado G., 2012b, MNRAS, 424, 3129 (SSMG)

Salvador-Solé E., Viñas J., Manrique A., Serra S., 2012a, MNRAS, 423, 2190

Sheth R. K., 2003, MNRAS, 345, 1200

Spitzer L., Jr, 1958, ApJ, 127, 17

Spitzer L., 1987, Dynamical Evolution of Globular Clusters. Princeton Univ. Press, Princeton, NJ

Springel V. et al., 2008, MNRAS, 391, 1685 (SWV)

Sugiyama N., 1995, ApJS, 100, 281

Taylor J. E., Babul A., 2001, ApJ, 559, 716

Taylor J. E., Babul A., 2004, MNRAS, 348, 811

Tollet É., Cattaneo A., Mamon G. A., Moutard T., van den Bosch F. C., 2017, MNRAS, 471, 4170

Tormen G., 1997, MNRAS, 290, 411

Tormen G., Diaferio A., Syer D., 1998, MNRAS, 299, 728

Tsallis C., 1988, J. Stat. Phys., 52, 479

van den Bosch F. C., Jiang F., 2016, MNRAS, 458, 2870

van den Bosch F. C., Ogiya G., Hahn O., Burkert A., 2018, MNRAS, 474, 3043

van den Bosch F. C., Tormen G., Giocoli C., 2005, MNRAS, 359, 1029

Viñas J., Salvador-Solé E., Manrique A., 2012, MNRAS, 424, L6

Wang J. et al., 2011, MNRAS, 413, 1373

Weinberg M. D., 1994, AJ, 108, 1398

Wetzel A. R., 2011, MNRAS, 412, 49

Zentner A. R., Berlin A. A., Bullock J. S., Kravtsov A. V., Wechsler R. H., 2005, ApJ, 624, 505

Zentner A. R., Bullock J. S., 2003, ApJ, 598, 49

APPENDIX A: FRACTION OF RELEASED SUBSUBHALOES

Dividing equation (18) by $\mathcal{N}^{\mathrm{tr}}(r, M_{\mathrm{s}}^{\mathrm{tr}})$ and defining $1 + f_{\mathrm{rel}}(r, M_{\mathrm{s}}^{\mathrm{tr}})$ as $\mathcal{N}^{\mathrm{stp}}(r, M_{\mathrm{s}}^{\mathrm{tr}})/\mathcal{N}^{\mathrm{tr}}(r, M_{\mathrm{s}}^{\mathrm{tr}})$, we have

$$1 + f_{\mathrm{rel}}\left(r, M_{\mathrm{s}}^{\mathrm{tr}}\right) = 1 + \int_{M_{\mathrm{s}}}^{M(r)} \mathrm{d}M\, \mathcal{N}^{\mathrm{acc}}(r, M) \left\langle \int_{R^{\mathrm{tr}}(v,r)}^{R(r,M)} \mathrm{d}r'\, \frac{\mathcal{N}_{[M,t(r)]}^{\mathrm{stp}}\left(r', M_{\mathrm{s}}^{\mathrm{tr}}\right)}{\mathcal{N}_{[M,t(r)]}^{\mathrm{tr}}\left(r', M_{\mathrm{s}}\right)} \frac{\mathcal{N}_{[M,t(r)]}^{\mathrm{tr}}\left(r', M_{\mathrm{s}}\right)}{\mathcal{N}^{\mathrm{tr}}\left(r, M_{\mathrm{s}}^{\mathrm{tr}}\right)} \right\rangle. \tag{A1}$$

The quantities $\mathcal{N}_{[M,t(r)]}^{\mathrm{stp}}(r', M_{\mathrm{s}}^{\mathrm{tr}})$ and $\mathcal{N}_{[M,t(r)]}^{\mathrm{tr}}(r', M_{\mathrm{s}}^{\mathrm{tr}})$ inside the integral on the right-hand side can be written in terms of the quantities $f_{\mathrm{rel}}(r')$ and $\rho(r')$ with subindex $[M, t(r)]$. All these quantities seen as functions of the scaled radius $\xi = r'/R(r, M)$ are universal, so we can change the subindex $[M, t(r)]$ by subindex $[M(r), t(r)]$ and, given the inside-out growth of the halo, by subindex $[M_{\mathrm{h}}, t_{\mathrm{h}}]$ or simply drop the subindex. (Of course, in this case, when rewriting the latter quantity as a function of the non-scaled radius, ξ must be multiplied by R_{h}.) After all those changes we have

$$1 + f_{\mathrm{rel}}\left(r, M_{\mathrm{s}}^{\mathrm{tr}}\right) = 1 + \int_{M_{\mathrm{s}}}^{M(r)} \mathrm{d}M\, \mathcal{N}^{\mathrm{acc}}(r, M)\, \frac{R^3(r, M)}{r^2} \left\langle \int_{Q_{v(v,r)}(v,r)}^{1} \mathrm{d}\xi\, \left[1 + f_{\mathrm{rel}}\left(\xi, M_{\mathrm{s}}^{\mathrm{tr}}\right)\right] \xi^2\, \frac{\mu(\xi)}{\mu(r)} \frac{\rho(\xi)}{\rho(r)} \right\rangle. \tag{A2}$$

Taking into account the relation (20) and the equality $R^3(r, M) = 3M/[4\pi\bar{\rho}(r)]$ (equation 3), equation (A2) can be written as

$$f_{\mathrm{rel}}\left(r, M_{\mathrm{s}}^{\mathrm{tr}}\right) \mu(r) = \frac{M(r) - M_{\mathrm{s}}}{M_{\mathrm{h}}\bar{\rho}(r)} \left\langle 3 \int_{Q_{v(v,r)}(v,r)}^{1} \mathrm{d}\xi\, \xi^2\, \left[1 + f_{\mathrm{rel}}\left(\xi, M_{\mathrm{s}}^{\mathrm{tr}}\right)\right] \mu(\xi)\, \rho(\xi) \right\rangle. \tag{A3}$$

For any given subhalo mass M_s^tr, equation (A3) holds for r satisfying the condition $M_\text{s}^\text{tr} \leq M(r)/3$. Near equality, where $\mathcal{N}^\text{acc}(r, M_\text{s}^\text{tr})$ vanishes, $f_\text{rel}(r, M_\text{s}^\text{tr})$ falls rapidly to zero and, over all the remaining radii, M_s in the denominator on the right-hand side of equation (A3) can be neglected. Thus, $f_\text{rel}(r, M_\text{s}^\text{tr})$ coincides for all subhalo masses M_s^tr and we can drop its argument M_s^tr. Lastly, by performing through partial integration the average over v on the right-hand side of equation (A3), we arrive at equation (23).

APPENDIX B: STRIPPING OF RELEASED SUBSUBHALOES

As shown in Section 4, the average over v of the Jacobian $\partial M_\text{s}^\text{tr}(v, r, M_\text{s})/\partial M_\text{s}$ is equal to the average over v of the $M^\text{tr}(v, r, M_\text{s})/M_\text{s}$ mass ratio, which only depends on r. Taking into account this relation for subsubhaloes with truncated mass M_s^tr released from first-level subhaloes into the intrahalo medium, we arrive, after integrating over the velocities v' in the host subhalo and v in the host halo at the following condition for a new tidal stripping to take place,

$$M^\text{tr,h} = \left\langle \left\langle \frac{\partial M_\text{s}^\text{tr,h}}{\partial M^\text{tr,s}} \right\rangle \right\rangle (r, r') \, M^\text{tr,s} = \left\langle \frac{\partial M^\text{tr,h}}{\partial M} \right\rangle (r) \left\langle \frac{\partial M}{\partial M^\text{tr,s}} \right\rangle (r') \, M^\text{tr,s}, \tag{B1}$$

where the extra index h or s going together with superindex s means that truncation takes place within the halo or the subhalo, respectively, r' is the apocentric radius of the subsubhalo within the host subhalo, and r is the apocentric radius of that subhalo (and of the released subsubhalo) within the host halo. The condition for a new tidal stripping is thus

$$\left\langle \frac{\partial M_\text{s}^\text{tr}}{\partial M_\text{s}} \right\rangle (r) < \left\langle \frac{\partial M_\text{s}^\text{tr}}{\partial M_\text{s}} \right\rangle (r'). \tag{B2}$$

The two partial derivatives are independent of the subsubhalo mass M_s. Since they refer to different hosts (to the halo that on the left-hand side and to the stripped subhalo that on the right-hand side), condition (B2) seems hard to assess. In the hypothetical case that the host subhalo accreted at $t(r)$ was identical to its host at that moment, the two partial derivatives would correspond to the same host at different radii, with r' smaller than r. Since stripping is more intense near the halo centre ($c(r) = c(M_\text{h}, t_\text{h}) R_\text{h}/r$), the partial derivative on the right-hand side (and the associated v-averaged mass ratio) would be smaller than that on the left-hand side. Consequently, condition (B2) would not be satisfied and there would be no new tidal stripping within the host halo (although there would still be repetitive stripping from that initial stripped configuration). Actually, accreted subhaloes are always less massive than the accreting host at the time of their accretion, so subhaloes are necessarily (slightly) more concentrated than the host and the stripping the subsubhalo suffers is stronger than the one it would suffer were the subhalo identical to the host at accretion. Therefore, there is no additional initial tidal stripping in the realistic case (just the usual repetitive stripping).

This conclusion holds, however, after averaging over v and v'. In the case that v' is very large, causing a very small stripping of the subsubhalo inside the subhalo host, and v is very small, causing a very marked stripping of the released subsubhalo inside the host halo, subsubhaloes will suffer a new stripping after being released in the intrahalo medium. But such a configuration should also likely cause the disruption of the released subhalo so that surviving subhaloes having undergone a new stripping after being released from the stripping of other subhaloes are expected to be very rare.

APPENDIX C: TANGENTIAL VELOCITY DISTRIBUTION FUNCTION

CUSP allows deriving the total (3D), radial and tangential velocity dispersion profiles of haloes (SSMG), but not their respective velocity distributions. Thus, to perform some explicit calculations, the averages over the tangential velocity of (accreted or stripped) subhaloes with apocentre at r have been performed using the (mass independent; Jiang et al. 2015) tangential velocity distribution function of the Tsallis (1988) form,

$$f_\text{t}(v, r) \propto v \left[1 + \frac{8v^2}{3\sigma^2(r)} \right]^{-5/2}, \tag{C1}$$

where $\sigma(r)$ is the 3D velocity dispersion profile, found for all particles in simulated haloes (Hansen et al. 2006).

Of course, this empirical distribution function must be adapted to our needs because it refers to all particles at r, while what we need is the distribution function for particles with apocentre at that radius. As orbiting particles spend most of the time near apocentre, the particles we are interested in dominate by far the total population at r. There are just a few more particles caught when they are crossing r from larger apocentric radii (i.e. they belong to accreted shells that were not yet virialized at the time $t(r)$). Although they are not numerous, these particles give rise to the otherwise null radial velocity dispersion at r. They also fill the tangential velocity distribution function (C1) beyond v_max, a region inaccessible to particles with apocentre at r, and likely also have a substantial contribution to that distribution function near v_max where the subhalo population with apocentre at r is small (Tormen 1997; Zentner et al. 2005; Wetzel 2011). However, at lower tangential velocities, particles with apocentre at r should clearly pre-dominate. Therefore, the velocity distribution of subhaloes and dark matter (DM) particles with apocentre at r should be well approximated by the Tsallis (1988) distribution function (C1) convolved with a Gaussian with central value equal to unity and 3σ equal to v_max. This is the approximate form we adopt. Remember that when the possibility of disruption is considered, the velocity distribution used to average over all *surviving* stripped subhaloes must also be taken null (in this case with a sharp cut-off) for $v < v_\text{dis}$.

Regarding the 3D velocity dispersion profile appearing in expression (C1), we could use that predicted by CUSP (SSMG). However, that velocity dispersion was derived for realistic triaxial haloes, while we are assuming here spherical symmetry. Thus we simply adopt the solution of the isotropic Jeans equation for spherically symmetric haloes endowed with the NFW profile with null boundary condition at infinity (Cole & Lacey 1996).

This paper has been typeset from a TeX/LaTeX file prepared by the author.